HHS Public Access

Author manuscript

Glia. Author manuscript; available in PMC 2019 March 01.

Published in final edited form as:

Glia. 2018 March ; 66(3): 623–636. doi:10.1002/glia.23269.

Sox2 Regulates Astrocytic and Vascular Development in the Retina

Amanda G. Kautzman[1,2], **Patrick W. Keeley**[1], **Michael M. Nahmou**[1,2], **Gabriel Luna**[1], **Steven K. Fisher**[1], and **Benjamin E. Reese**[1,2]

[1]Neuroscience Research Institute, University of California at Santa Barbara, Santa Barbara, CA 93106-5060

[2]Department of Psychological and Brain Sciences, University of California at Santa Barbara, Santa Barbara, CA 93106-5060

Abstract

Sox2 is a transcriptional regulator that is highly expressed in retinal astrocytes, yet its function in these cells has not previously been examined. To understand its role, we conditionally deleted *Sox2* from the population of astrocytes and examined the consequences on retinal development. We found that *Sox2* deletion does not alter the migration of astrocytes, but it impairs their maturation, evidenced by the delayed upregulation of glial fibrillary acidic protein (GFAP) across the retina. The centro-peripheral gradient of angiogenesis is also delayed in Sox2-CKO retinas. In the mature retina, we observed lasting abnormalities in the astrocytic population evidenced by the sporadic loss of GFAP immunoreactivity in the peripheral retina as well as by the aberrant extension of processes into the inner retina. Blood vessels in the adult retina are also under-developed and show a decrease in the frequency of branch points and in total vessel length. The developmental relationship between maturing astrocytes and angiogenesis suggests a causal relationship between the astrocytic loss of *Sox2* and the vascular architecture in maturity. We suggest that the delay in astrocytic maturation and vascular invasion may render the retina hypoxic, thereby causing the abnormalities we observe in adulthood. These studies uncover a novel role for *Sox2* in the development of retinal astrocytes and indicate that its removal can lead to lasting changes to retinal homeostasis.

Keywords

Astrocyte; Angiogenesis; Blood vessels; Collagen; GFAP; Vasculature

Introduction

Astrocytes play many roles in the developing and mature central nervous system (CNS), including the retina. They promote growth and maturation of neuronal cells by stimulating synaptogenesis and axon growth (Allen et al., 2012; Barker & Ullian, 2008; Christopherson et al., 2005; Ullian, Sapperstein, Christopherson, & Barres, 2001), secrete growth factors

Address correspondence to: B.E. Reese, Neuroscience Research Institute, UC Santa Barbara, Santa Barbara, CA 93106-5060. Phone: 805-893-2091.

necessary for neuronal differentiation and survival (Banker, 1980; Liesi & Silver, 1988), aid in synaptic pruning (Stevens et al., 2007), and buffer ions in the extracellular space (Newman, 1986). Within the retina, the stellate morphology of the astrocytes forms a web-like network of overlapping processes that use gap-junctions to propagate intracellular signals and establish metabolic homeostasis (Hollander et al., 1991; Ramirez, Trivino, Ramirez, Salazar, & Garcia-Sanchez, 1996). Astrocytes also play an important role in the vascularization of the retina (Dorrell, Aguilar, & Friedlander, 2002; Dorrell et al., 2010; O'Sullivan et al., 2017), providing a scaffold for blood vessels to follow as they migrate from the optic nerve head (ONH) across the inner surface of the retina via the secretion of growth factors such as vascular endothelial growth factor (VEGF).

Astrocytes constitute the majority of cells in the CNS (Molofsky et al., 2012), yet surprisingly little is known about the genetic factors that regulate their development. Transcriptome analysis performed on purified populations of astrocytes derived from mouse cortical tissue found *Sox2* to be within the top 10% of all expressed genes (Cahoy et al., 2008). In addition, *Sox2* expression is enriched in astrocytes, being expressed at higher levels than in cortical neurons and other glial cells (Cahoy et al., 2008; Zhang et al., 2014). In the retina, Sox2 is only expressed within three cellular populations, cholinergic amacrine cells, Müller glia, and astrocytes, being the most abundant within the astrocytic population (Whitney et al., 2014; Macosko et al., 2015). *Sox2* belongs to the large SRY-related HMG-box transcription factor family and is best recognized for its role in early development by maintaining embryonic stem cell pluripotency (Matsushima, Heavner, & Pevny, 2011; Taranova et al., 2006). *Sox2* is also a critical gene for eye development as mutations in humans lead to severe abnormalities in eye formation (Fantes et al., 2003; Schneider, Bardakjian, Reis, Tyler, & Semina, 2009). In addition, it has been suggested that *Sox2* is able to promote glial cell survival in cultures of dorsal root ganglion cells (Koike, Wakabayashi, Mori, Hirahara, & Yamada, 2015). Given these documented roles for *Sox2*, the present study has assessed its role in the development of retinal astrocytes.

Using a conditional deletion strategy to excise *Sox2* from the population of retinal astrocytes, we examined the consequences for astrocytic and vascular development, and for the astrocytic and vascular architecture in maturity. While we found no alteration in the spatio-temporal time-course of astrocyte migration across the retina, we observed a conspicuously delayed expression of glial fibrillary acidic protein (GFAP), a hallmark of their maturation. Vascular invasion across the retinal surface was also delayed. In maturity, the adult retina exhibited an aberrant distribution of astrocytic processes as well as vascular network abnormalities, yet the overall architecture of the retina was unaffected. These data identify *Sox2* as an important participant in the development of astrocytes, and suggest a complex interaction with the forming vasculature in the mouse retina.

Materials and Methods

Animals

GFAP-Cre (FVB-Tg(GFAP-cre)25Mes/J) mice and *Sox2-flox* mice (Sox2$^{tm1.1Lan}$/J) were used to generate conditional knockout mice (CKO) in which GFAP-positive astrocytes lack expression of *Sox2*. Cre activation was characterized by crossing *GFAP-Cre* mice with a

reporter mouse carrying a floxed stop-cassette upstream of *EYFP*, under a constitutively active promoter (*Rosa- EYFP;* B6.129X1-Gt(ROSA)26Sor$^{tm1(EYFP)Cos}$/J); Cre is activated in almost all astrocytes and a subset of Müller glia (data not shown). This was additionally confirmed by immunostaining retinas for Cre recombinase (Figure S1). All *GFAP-Cre* control animals (CTL) were CKO littermates that lacked *GFAP-Cre* and/or *Sox2-loxP* alleles. All three lines of mice were obtained from The Jackson Laboratories (Bar Harbor, MA; *GFAP-Cre*: #004600; *Sox2-flox*: #013093; *Rosa-EYFP*: #006148). Retinas were examined from post-natal mice, and into maturity, with retinas older than 21 days of age designated as adult retinas. All experiments were conducted under authorization by the Institutional Animal Care and Use Committee at the University of California–Santa Barbara and in accordance with the National Institutes of Health *Guide for the Care and Use of Laboratory Animals* and the ARVO Statement for the Use of Animals in Ophthalmic and Vision Research.

Tissue preparation

Mice were given a lethal injection of sodium pentobarbital (120 mg/kg, i.p.) and, once deeply anesthetized, were intracardially perfused with 2 ml of saline followed by ~50 ml of 4% paraformaldehyde dissolved in sodium phosphate buffer (pH 7.2, at 20°C). Whole retinas were subsequently dissected from eyes and processed for wholemount preparations or cut into 150 μm on a Vibratome. Particular care was taken to prevent damage to the inner surface of the retina during dissection.

Immunostaining

Dissected wholemount retinas or sections were incubated in 5% normal donkey serum in phosphate-buffered saline (PBS) with 1% Triton-X for three hours. They were then rinsed in PBS and incubated in primary antibodies diluted in PBS with 1% Triton-X for 72 hrs. Primary antibodies used in this study are listed in Table 1. In addition, Hoechst (Invitrogen, Eugene, OR; 1:1000), NeuroTrace 530/615 (ThermoFisher Scientific, Waltham, MA; #N21482, 1:500) and PNA lectin conjugated to Alexa Fluor 647 (ThermoFisher Scientific, Waltham, MA; #L32460, 1:500) were used and added to the solution of primary antibodies. Retinas were subsequently rinsed in PBS and incubated overnight in the secondary antibodies. All secondary antibodies were raised in donkey and conjugated to AlexaFluor dyes (Jackson ImmunoResearch Laboratories, West Grove, PA; 1:200). All steps were conducted under agitation at 4°C.

Image acquisition

Adult wholemount retinal images were assembled from ~250 40× maximum projection fields stitched together using Imago 1.5 (Mayachitra Inc., Santa Barbara, CA) to create a single high-resolution image of the entire retina. Postnatal retinal images were comprised of ~18 10× maximum projection fields similarly stitched together. Each projection was taken from ~40 optical sections at 1 μm intervals through the z-axis. For the analysis of astrocytic sprouting, large fields (0.81 mm^2) were made by stitching 16 individual 40× z-stacks at 4 different locations on the retina, one per quadrant. All images were acquired on an Olympus FV1000 scanning laser confocal microscope.

Quantification of retinal ganglion cells, microglia, and Cre-positive cells

Retinal ganglion cells, identified as Brn3b-positive profiles in the ganglion cell layer (GCL), were counted from confocal micrographs of 8 peripheral and 4 central fields (0.09 mm^2) per animal (CTL: n = 6; CKO: n = 5) using Fiji software (https://fiji.sc/). Microglia, identified as Iba1-positive profiles in both the GCL and the inner nuclear layer (INL) (Schafer et al. 2012), were counted from 4 peripheral and 4 central fields (0.18 mm^2) per animal (CTL: n = 4; CKO: n = 5) using BioQuant Nova Software (BIOQUANT Image Analysis Corporation, Nashville, TN). Confocal micrographs of 4 peripheral and 4 central fields (0.10 mm^2) were taken from 3 CTL retinas, to identify all Cre-positive, Sox9-positive, and double-labeled cell bodies in the GCL and nerve fiber layer (NFL) using Fiji software.

Quantification of astrocytic sprouting

Z-stack projection images extended into the inner retina to include all GFAP-positive staining, excluding labeling in the NFL. Images were contrast-enhanced in Adobe Photoshop (San Jose, CA). Fiji software was used to automatically threshold every labeled profile in the inner retina and the number of pixels that are GFAP-positive across each 0.81 mm^2 field were quantified. Counts were averaged to yield values per retina and represented as fold changes over CTL for visualization purposes. A two-tailed Mann-Whitney U test was used to test for differences between the two groups using the raw data (U = 12, n1 = 8, n2 = 9) with a threshold for statistical significance of $p \leq 0.05$. Orthogonal reconstructions were made from 60× z-stacks extending 120 μm into the retina. Supplementary videos 1 (CTL) and 2 (CKO) were made from these stacks at 20 frames per second.

Quantification of astrocytic and vascular extension

Measurements of the extension of the GFAP-positive astrocytic network and collagen-positive vascular network toward the retinal periphery were made from 4 locations across the developing retina, one in each quadrant. The distance of immunopositive profiles was calculated as a percentage of the distance from the ONH to the retinal margin at each location, and subsequently averaged across the quadrants for each retina. Extreme outliers (Q3 + 3*IQR, Q1 – 3*IQR) were removed. Differences at each time point were assessed using a two-tailed Mann-Whitney U test with a threshold for statistical significance = $p \leq 0.05$ (GFAP P5: $U = 3$, n1 = 4, n2 = 4; GFAP P10: $U = 1$, n1 = 4, n2 = 5; Collagen P5: $U = 2$, n1 = 4, n2 = 5; Collagen P10: $U = 0$, n1 = 5, n2 = 5; Collagen Adult: $U = 3$, n1 = 5, n2 = 5).

Quantification of the vascular network

Vascular branch points were counted manually from 8 peripheral and 4 central fields (0.09 mm^2) per animal using Fiji software. A branch point was defined as any intersection of two blood vessels, excluding small capillaries. Total vessel length was also measured from the same fields by tracing all Collagen IV-positive vessels per field and summing them. The 12 measurements were averaged to yield values for each retina, and a two-tailed student's t-test was performed, using a threshold for statistical significance of $p \leq 0.05$.

All quantification was conducted without knowledge of genotype, with either the retinas or confocal micrographs being coded and randomly intermingled beforehand.

Results

Characterization of the Sox2-CKO retina

The conditional deletion of *Sox2* from retinal astrocytes was confirmed in the mature retina by the absence of Sox2 immunoreactivity from all retinal astrocytes. GFAP-positive astrocytes remain present (yellow arrowheads in Figure 1a,e), but they have now lost their Sox2-immunoreactivity in the CKO retina, while those in littermate control retinas remain Sox2-positive (compare yellow arrowheads in Figure 1b,1f). Sox2-immunopositive cells remain in the CKO retinas (white arrows in Figure 1f), however, each one of these cells was confirmed to be a cholinergic amacrine cell, also observed in control retinas (white arrows in Figure 1c,g). Furthermore, nearly all cell bodies (98%) residing in the nerve fiber layer that are Cre recombinase (Cre)-positive are also immuno-positive for Sox9, being another astrocytic marker expressed exclusively by astrocytes and Müller glia in the retina (Macosko et al., 2015), confirming their status as astrocytes (Figure S1a–e). In addition, 93% of Sox9-positive astrocytes were also Cre-positive (Figure S1f). But for the occasional Cre-positive astrocyte astride a blood vessel, the populations of endothelial cells and pericytes that exclusively associate with blood vessels are not Cre-positive (Figure S1g–j). These combined results confirm the selectivity of the loss of Sox2 from the population of astrocytes in CKO retinas. All other features of the mature retinal architecture appear unaltered, evidenced by immunolabeling retinal sections with antibodies to reveal the cellular and synaptic lamination (Figure S2).

Sox2-deficient astrocytes exhibit a delayed maturation

We first investigated whether the loss of *Sox2* in astrocytes causes a disruption to their development. Immature astrocytes expressing Sox2 migrate into the retina from the ONH shortly before the day of birth, by responding to environmental cues such as platelet-derived growth factor A-chain (PDGF-A) (Fruttiger et al., 1996), laminins β2 and γ3 (Gnanaguru et al., 2013), and the axons of retinal ganglion cells (Distler, Dreher, & Stone, 1991; O'Sullivan et al., 2017). These immature astrocytes, visualized by expression of Pax2, migrate radially across the retinal surface, reaching the peripheral edge of the retina by postnatal (P) day 5 (Chu, Hughes, & Chan-Ling, 2001; Chan-Ling, Chu, Baxter, Weible Li, & Hughes, 2009; Ling, Mitrofanis, & Stone, 1989; Sandercoe, Madigan, Billson, Penfold, & Provis, 1999; Stone & Dreher, 1987; Watanabe & Raff, 1988). At P1, migrating Pax2-positive astrocytes are found in both CTL and CKO retinas with no apparent differences in their spatial distribution nor in their morphologies (Figure 2a–d). These cells, also expressing Sox9 on P1, are found in comparable densities, extending from the ONH roughly two-thirds to the distance to the peripheral margin of the retina (compare Figures 2i with 2j), coursing across the NFL. In the CTL retina, these migrating astrocytes are Sox2-immunopositive (Figure 2e), yet in the CKO retina their Sox2-positive status is no longer detected (Figure 2g). Note that a few cells remain Sox2-immunoreactive in the CKO retina (white arrows in Figure 2g); these cells have a smaller and rounder profile, not unlike those that are distributed in the GCL, being the cholinergic amacrine cells (Figure 2f,h). These are also present in the control retina at P1 (white arrows in Figure 2e), but are generally obscured by the more conspicuous Sox2-positive population of astrocytes therein. That these few Sox2-positive cells in the CKO retinas are in fact cholinergic amacrine cells displaced closer to the NFL is

evidenced by the presence of weak ChAT-immunoreactivity in their cytoplasm (Figure 2e′,e″,g′,g″). The Pax2-positive cells continue their migration toward the periphery by P5, in both CKO and CTL retinas (to the right in Figures 3a,d). These data confirm the loss of Sox2 from the population of astrocytes during their period of migration across the developing retina, yet demonstrate no obvious disruption in their migratory progress toward the retinal periphery.

Astrocytes express GFAP at low levels during the perinatal period as they invade the retina (West, Richardson, & Fruttiger, 2005), but gradually increase expression throughout postnatal development until expression plateaus around P10 (Sarthy, Fu, & Huang, 1991; Tao & Zhang, 2014), when Pax2 labeling of astrocytes gradually subsides. Coincident with this transition, the spatial distribution of the astrocytes changes by P5, in association with the emerging vasculature. At this age, these Pax2-positive cells closest to the ONH form ring-like patterns associated with the emerging vasculature and exhibit heavy GFAP expression, diminishing toward peripheral regions already colonized by less mature astrocytes (Figure 3a–c). In comparison, CKO retinas exhibit less GFAP extension towards the peripheral edge than CTL retinas, despite the widespread distribution of astrocytes evidenced by their Pax2 immunoreactivity (Figure 3d–f, i), though this difference did not reach statistical significance at P5 ($p = 0.149$). These Pax2-positive astrocytes in the more central regions of the CKO retina also lack the ring-like formations seen in CTL retinas.

By postnatal day 10, when Pax2 is no longer detected in retinal astrocytes, both CTL and CKO astrocytes robustly express GFAP (Figure 3g,h), yet there remains a significant delay in GFAP upregulation peripherally (compare white arrowheads with red dashed line indicating the retinal margin in Figure 3g,h; Figure 3j, $p = 0.027$). This delay, however, is a transitory feature in the CKO retina, ultimately giving way to the characteristic pattern of astrocytes blanketing the mature retina (see below). Note as well that the transition to the thin web-like patterning seen in maturity is already beginning to materialize in the CTL retinas (Figure 3g), while this is notably delayed in the CKO retinas. GFAP-processes in the P10 CKO retinas exhibit a morphology that outlines the emerging vasculature, existing as thicker bundles of processes, not unlike that in the central retina in P5 CTLs (Figure 3b,h). Taken together, the data from these developmental time-points indicate that Sox2 plays a key role in the maturation of astrocytes in the developing retina.

Adult astrocytes exhibit morphological abnormalities

To assess whether these developmental abnormalities might translate into lasting changes within the population of mature astrocytes, we examined retinas from adult animals for perturbations to the mature astrocytic network. Control retinas exhibit a uniform GFAP staining pattern across all retinal eccentricities (Figure 4a). High magnification images reveal the typical web-like network of thin stellate processes that appear evenly distributed (Figure 4a′). Conversely, CKO retinas show a profound, if sporadic, loss of GFAP staining specifically in peripheral regions, appearing unaffected at central locations (Figure 4b,b′). The severity of this phenotype varies amongst CKO animals, ranging from a single peripheral patch to almost the entirety of the peripheral retina. In those peripheral regions with such atypical GFAP immunolabeling, remaining astrocytic processes show a loss of the

characteristic web-like distribution of processes when compared to CTL astrocytes (Figure 4a′,b′). This depletion in the pattern of GFAP labeling was observed in 23/28 quadrants when sampling across seven CKO retinas, never having been observed in CTL retinas (Figure S3). However, some quadrants remain unaltered, indicating that astrocytes are capable of migrating to the retinal margin in CKO animals. That they had done so, earlier in development in these affected quadrants, is supported by the observation that the retinal vasculature is present in these depleted regions (Figure S3d,d′). These results suggest that the depleted territory reflects a regressive event but whether it is due to an abnormal loss of GFAP immunoreactivity or apoptosis of the astrocytes themselves, is unclear.

The processes of wildtype astrocytes, labeled with GFAP, are normally restricted to the retinal NFL, with little to no labeling extending into the inner retina (Figure 5a–d). In injury conditions however, like that of retinal detachment, mouse astrocytes have been shown to extend processes into the inner retina (Luna et al., 2016). In regions of the CKO retina removed from the astrocytic deficit, we observed aberrant astrocytic sprouting into the inner plexiform layer (IPL), well beyond the normal stratified distribution within the NFL (Figure 5e–h). These retinas exhibit, on average, an eight-fold increase in the density of processes extending into the IPL compared to controls, albeit CKO samples showed conspicuous variability (Figure 5i, $p = 0.012$). These sprouted processes in CKO retinas can extend over a hundred microns into the retina and appear to stratify at particular depths as seen in high magnification z-stack reconstructions from 120 μm thick stacks from CTL and CKO retinas (Figure 5j,k; Supplemental Videos 1 and 2). These processes are invariably traced to astrocytes in the inner retina, and are not associated with the Müller glia. Indeed, sectioned retinas show the Vimentin-positive architecture to be unchanged in the CKO retinas (Figure S4a,b), and double-labeling with GFAP confirms that none of these sprouted processes in the CKO retinas are Vimentin-positive (Figure S4c,d).

Despite the sporadic absence of peripheral GFAP and this aberrant sprouting of processes into the inner retina elsewhere, other assessments of retinal histology (e.g. Figure S2), including retinal area (Figure S5a), appear unchanged between CTL and CKO retinas. However, in a few rare cases, we observed large regions lacking GFAP labeling (Figure S5e, compare with S5c) and a reduction in the density of retinal ganglion cells and their axons labeled with antibodies to Neurofilaments, the severity of which never mapped precisely upon the changes in the astrocytic array (Figure S5f, compare with S5d). When analyzing mature retinas without biasing our sampling protocol to depleted regions, CKO retinas exhibited a slight, if non-significant, reduction in the density of Brn3b-positive retinal ganglion cells compared to CTLs (Figure S5b). Because of such rare extreme examples showing depleted Neurofilament-positive retinal ganglion cells (e.g. Figure S5f), the Brn3b+ cell counts are likely indicative of a slight reduction in ganglion cell density. Counts of Iba1+ microglia, at P17, sampled without biasing to astrocyte-depleted regions, show a similar slight, if non-significant, increase in their frequency, restricted to the GCL (Figure S6a–c), which may be indicative of an apoptotic loss of these RGCs, or possibly the astrocytic changes noted above. That the astrocytes have died in those regions depleted of GFAP labeling is supported by the observation that another marker for astrocytes, Sox9, is similarly missing from those depleted regions (Figure S7a–i), but it remains a possibility that they have simply down-regulated Sox9 expression. Nevertheless, these results would suggest

that, despite the complete loss of Sox2 from the entire astrocytic population, these retinas rarely show conspicuous changes or other histological signs of severe degeneration (e.g. Figure S2). Rather, the pattern of mature astrocytes shows only a regional loss as well as aberrant sprouting, suggesting a modest level of cellular stress that, in more extreme cases, impacts the population of neurons most intimately associated with the astrocytes.

CKO retinas exhibit delays in vascular growth

It is known that as astrocytes enter the retina, they secrete many factors, including VEGF, which serve as migratory guides for endothelial tip cells residing on the leading edge of the developing retinal vasculature (Fruttiger, 2002; Jiang, Bezhadian, & Caldwell, 1995; Zhang et al., 2014). The apparent delay in astrocyte maturation suggested a potential effect upon the maturation of the vasculature itself. Indeed, the normal invasion of the vasculature, from the ONH to the retinal periphery, was conspicuously delayed compared to that of controls, as evidenced by the pattern of Collagen IV immunostaining in whole retinas (Figure 6a–g). At P5, the developing retinal vasculature in CTL retinas extends from the ONH to roughly 55% of the distance to the peripheral margin. In the more central regions, this web of maturing vessels contours nicely with the ring-like pattern of astrocytes at this same age (compare with Figure 3c). By contrast, the developing retinal vasculature is delayed in the CKO retinas, having extended only 33% of this centro-peripheral dimension (Figure 6a,d,g, $p = 0.050$). By P10, the CKO vasculature continues to show a delay in advancement towards the retinal margin, extending only to 92%, compared to 99% in CTL retinas (Figure 6b, $p = 0.009$). CKO retinas, interestingly, show a lasting significant if slight reduction in the establishment of the vascular network at the very peripheral margin of the retina in adulthood compared to controls (Figure 6c,f,g, $p = 0.047$).

Given the sprouting observed in the population of mature astrocytes in CKO retinas, we examined other features of the mature vascular network in further detail. But with one exception (Figure S5g), the CKO vasculature showed no gross morphological differences from control animals, aside from the above-mentioned absence at the extreme margin of the retina (Figure 6c,f,g); detailed analysis, however, revealed subtle changes to the vascular architecture, pervasive throughout the retina (Figure 6h,i). CKO retinas have significantly fewer vascular branch points than controls (Figure 6j, $p = 0.002$). Abnormal blood vessel branching is thought to result from a disordered development of the retinal angioarchitecture (DiMaio & Sheibani, 2008), implying that CKO animals have impairments in the formation of their vascular network causing a subsequent decrease in the number of vascular branch points. This was corroborated by the CKO retinas showing a significant decrease in overall vessel length when compared to fields from CTL retinas (Figure 6k, $p = 0.006$). These results suggest that the delayed arrival of the retinal vasculature may impede normal vascular branch formation, resulting in a lasting diminution of the vascular architecture, raising the possibility that the CKO retina might be mildly anoxic during development and in maturity.

Discussion

Here we identify a novel role for the transcription factor Sox2 in the development of retinal astrocytes and vasculature. We show that Sox2 is necessary for the time course of astrocytic

maturation in early postnatal development, as well as for the establishment and/or maintenance of astrocytic morphology in adulthood, evidenced by the regional loss of GFAP expression and aberrant sprouting into the inner retina after its removal. Vascular invasion into the retina in these CKO animals is also delayed and defects to the vascular network are present in adulthood.

To our knowledge this is the first evidence that Sox2 plays a role in astrocytic development and one of the few instances of a role for the gene outside of very early embryonic development. In addition, very few studies have examined the role of Sox2 specifically in retinal tissue. Recently, *Sox2* was shown to be expressed, uniquely amongst retinal neurons, in the cholinergic amacrine cell population, where its conditional deletion affected the positioning of cholinergic somata and the stratification of their dendrites (Whitney et al., 2014). *Sox2* has also been shown to be critical for developing Müller glia, as its conditional deletion from these cells alters their progenitor capacity and cellular morphology (Bachleda, Pevny, & Weiss, 2016; Surzenko, Crowl, Bachleda, Langer, & Pevny, 2013). The present study now highlights new roles for this transcription factor in retinal astrocytes, the only other cellular population expressing Sox2 in the mature retina. Taken together these studies show that Sox2 plays a different role postnatally than it does during early embryonic development, notably by influencing cellular maturation and morphology.

Sox2 is required for astrocytic maturation

Sox2 is a highly conserved transcriptional regulator of stem cell pluripotency, and is well known to play an essential role in all stages of CNS development in mammals (Kiefer, 2007). As astrocyte precursor cells mature, they downregulate genes such as *Pax2* and *Vimentin* while concurrently upregulating *GFAP* and *S100b*, among others (reviewed in Tao & Zhang, 2014). While it is known that Sox2 is present in astrocyte precursor cells and in mature astrocytes, how it interacts with other genes, in cells other than neural stem cells, remains to be determined. Our data implicate *Sox2* as essential for astrocytic maturation as evidenced by the delayed upregulation of GFAP when *Sox2* is genetically removed from developing astrocytes.

We confirmed that Sox2 was removed from astrocytes by the day of birth, and while Cre-mediated excision of Sox2 occurred prior to the normal upregulation of *GFAP*, we suspect this could be due to differential regulation of the *GFAP-Cre* transgene compared to the endogenous *GFAP* promoter. Cre expression appears to be consistent with the endogenous localization of GFAP, however, since almost all Cre-positive cells in the NFL of the adult retina were determined to be astrocytes, and almost all astrocytes were determined to be Cre-positive (Figure S1). Furthermore, these astrocytes were shown to be Sox2-negative in CKO retinas, while the population of cholinergic amacrine cells remained Sox2-positive (Figures 1,2).

Sox2 likely plays a role in cellular maintenance, given the observed regional loss of astrocytes and their atypical sprouted morphology in the mature retina. Sox2 is traditionally regarded as a transcriptional activator, although more recent studies have suggested that Sox2 can function as a repressor in neural stems cells (Liu et al., 2014). Indeed, Sox2 has been reported to repress the *GFAP* promoter *in vitro*, although it is known that genes can act

as both activators and repressors depending on the tissue and cell type they are expressed in, as well as the availability of cofactors (Liu et al., 2014). Those studies would suggest that *GFAP* may be an activational target of Sox2, either directly, or indirectly. That *GFAP* is eventually upregulated shows that other factors must participate; despite this, the lasting changes make clear the critical role for *Sox2* expression at a particular developmental stage for normal astrocytic maturation.

Sox2 removal from astrocytes delays retinal vascularization

It has been postulated that astrocyte maturation, indexed by GFAP upregulation, could result from the heightened availability of oxygen following angiogenesis (West et al., 2005; Zhang, Porat, Alon, Keshet, & Stone, 1999). In the present study, we observed a delay in vascularization following the removal of Sox2 from astrocytes. Given that vessels spread radially across the retinal surface following factors produced by astrocytes, a likely hypothesis is that Sox2-deficient astrocytes may alter this process leading to abnormal angiogenesis.

Developing astrocytes are known to secrete VEGF (Chan-Ling & Stone, 1991; West et al., 2005) in response to the hypoxic conditions present before tissue vascularization has taken place (Provis et al., 1997; West et al., 2005). Endothelial tip cells, at the leading edge of the developing vascular network, express the VEGF receptor VEGFR2 (Gerhardt et al., 2003). Their activation by VEGF has been shown to promote their extension towards the retinal periphery (Dorrell et al., 2002; Gerhardt et al., 2003; Ruhrberg et al., 2002; Stone et al., 1995; West et al., 2005). This arrival of blood vessels brings oxygen and therefore reduces the anoxic state. As it has been proposed that the availability of oxygen itself may trigger the maturation of the astrocytes (including the upregulation of GFAP) (West et al., 2005; Zhang et al., 1999), the present results suggest that the role of Sox2 is a complex and likely indirect one, and implicates VEGF as a potential upstream player. Our data show that CKO astrocytes migrate into the retina normally, evidenced by Pax2-positive and Sox9-positive profiles being present at early postnatal stages; however, angiogenesis and astrocytic maturation are delayed. Astrocytes deprived of Sox2 may be deficient at initiating angiogenesis in response to the initial hypoxic conditions (due to a deficiency in VEGF signaling), thereby causing the delay in oxygenation of the retina, consequently leading to the delay in GFAP upregulation. Further experiments are needed to determine if Sox2-deficient astrocytes are unable to sense and/or properly respond to a hypoxic environment and therefore alter their secretion of angiogenic-promoting factors like VEGF.

Although unlikely, it is possible that the delayed astrocytic maturation and the delay in angiogenesis that we observe are the result of two separate processes. It has been shown that factors other than VEGF play a role in the interplay between astrocyte and vascular development of the retina. For example, leukemia inducing factor (LIF) expression by endothelial cells is believed to inhibit astrocytic VEGF expression and promote GFAP activation, thereby promoting maturation of astrocytes (Kubota, Hirashima, Kishi, Stewart, & Suda, 2008; Kubota & Suda, 2009; Mi, Haeberle, & Barres, 2001; Nakashima, Yanagisawa, Arakawa, & Taga, 1999). The astrocytic deletion of *Sox2* could cause a delayed

maturation by indirectly decreasing LIF production, for example, to further impede astrocytic maturation.

Astrocytic and vascular aberrations in the mature retina

While there is strong evidence for the interaction between astrocytes and blood vessels in development as previously described, less is known about their relationship in mature animals. In this study we have not only uncovered a role for Sox2 in the developing retina but observe permanent aberrations to the astrocytic and vasculature networks in the mature retina as well. CKO retinas show a regional loss of GFAP immunoreactivity at peripheral locations, yet this has never been observed at central eccentricities near the ONH. Curiously, this regional difference is only observed for this specific phenotype; the astrocytic sprouting, as well as changes to the vasculature, occur at all locations across the retinal surface.

Given our observation that angiogenesis is delayed in CKO animals, this suggests that the peripheral retina may experience a prolonged period of anoxia, in turn further impacting the maturation of the astrocytes, perhaps by the diminished availability of other factors. While speculative, it appears plausible given the sustained interaction, both physical and metabolic, between astrocytes and blood vessels in the mature animal (reviewed in Sofroniew & Vinters, 2010).

We first observe the peripheral loss of GFAP labeling around P15, yet it appears in all CKO animals by P21. The extent of these depleted regions is not age-dependent; older animals do not exhibit more quadrants or larger peripheral patches with GFAP loss. This implies that the diminution of GFAP in the peripheral retina is not a severe degenerative phenotype but instead a consequence of an earlier developmental deficit. Immunostaining for an alternative astrocytic marker, Sox9, yields no evidence for astrocytes remaining within GFAP-deficient peripheral patches (Figure S7). While this result might suggest that astrocytes have undergone apoptosis in these regions, it is conceivable that they have simply lost these differentiated features of astrocytes, and are therefore unrecognizable when labeling for GFAP or Sox9. This is not so implausible when considering the loss of cellular identity when Sox2 is removed from cholinergic amacrine cells in the retina; while these cells retain their cholinergic status, they lose other features that discriminate between the ON versus OFF populations, including the loss of monostratified dendritic arbors in the ON population, and the loss P2X2 receptor labeling in the OFF population (Whitney et al., 2014).

What remains to be elucidated is how the aberrant astrocytic sprouting relates to our other described adult phenotype, namely that of the peripheral GFAP loss. It has been previously reported that in mouse models of retinal detachment, astrocytes not only sprout into the neural retina but also upregulate GFAP (Luna et al., 2016). In this injury condition, remodeled astrocytic processes follow blood vessels into the inner retina, yet in our CKO retinas we have not observed any obvious correlation. In addition, we do not observe any upregulation of GFAP, rather the opposite, implying that different processes control the two astrocytic phenotypes we describe. Conversely, the loss of Sox2 could create an intrinsic level of cellular stress thereby causing some astrocytes to undergo apoptosis, perhaps in regions providing less trophic support, while causing others to remodel by aberrantly extending their processes.

We observed a less complex superficial blood vessel network in CKO retinas, by measures of branch point frequency and vessel length. We believe this to be a lasting result of the delay in angiogenesis, yet it could be due to a remodeling of the network after reaching the retinal margin. Other groups have argued that if vascular branch points are decreased then overall vessel length should increase conversely (Giocanti-Auregan et al., 2016), yet we observe a significant decrease in both. This indicates a general underdevelopment of the vascular network. In severely astrocyte-depleted patches we have observed substantial aberrations to blood vessel patterning, i.e. the appearance of tortuous thickened vessels lacking finer capillary networks (Figure S3g). Most CKO retinas did not exhibit conspicuous abnormalities such as this, yet all showed an overall diminution of the superficial vascular plexus (Figure 6f,j,k). Taken together these data implicate *Sox2* as an important if indirect player in the development of the vascular network, mediated by the retinal astrocytes.

Supplementary Material

Refer to Web version on PubMed Central for supplementary material.

Acknowledgments

This research was supported by the National Institutes of Health (R01 EY019968; S10 OD010610).

References

Allen NJ, Bennett ML, Foo LC, Wang GX, Chakraborty C, Smith SJ, Barres BA. Astrocyte glypicans 4 and 6 promote formation of excitatory synapses via GluA1 AMPA receptors. Nature. 2012; 486(7403):410–414. DOI: 10.1038/nature11059 [PubMed: 22722203]

Bachleda AR, Pevny LH, Weiss ER. Sox2-Deficient Muller Glia Disrupt the Structural and Functional Maturation of the Mammalian Retina. Invest Ophthalmol Vis Sci. 2016; 57(3):1488–1499. DOI: 10.1167/iovs.15-17994 [PubMed: 27031842]

Banker GA. Trophic interactions between astroglial cells and hippocampal neurons in culture. Science. 1980; 209(4458):809–810. [PubMed: 7403847]

Barker AJ, Ullian EM. New roles for astrocytes in developing synaptic circuits. Commun Integr Biol. 2008; 1(2):207–211. [PubMed: 19513261]

Cahoy JD, Emery B, Kaushal A, Foo LC, Zamanian JL, Christopherson KS, … Barres BA. A transcriptome database for astrocytes, neurons, and oligodendrocytes: a new resource for understanding brain development and function. J Neurosci. 2008; 28(1):264–278. DOI: 10.1523/JNEUROSCI.4178-07.2008 [PubMed: 18171944]

Chan-Ling T, Stone J. Factors determining the morphology and distribution of astrocytes in the cat retina: a ‘contact-spacing’ model of astrocyte interaction. J Comp Neurol. 1991; 303(3):387–399. DOI: 10.1002/cne.903030305 [PubMed: 2007656]

Chan-Ling T, Chu Y, Baxter L, Weible M II, Hughes S. In vivo characterization of astrocyte precursor cells (APCs) and astrocytes in developing rat retinae: Differentiation, proliferation, and apoptosis. Glia. 2009; 57:39–53. DOI: 10.1002/glia.20733 [PubMed: 18661555]

Christopherson KS, Ullian EM, Stokes CC, Mullowney CE, Hell JW, Agah A, … Barres BA. Thrombospondins are astrocyte-secreted proteins that promote CNS synaptogenesis. Cell. 2005; 120(3):421–433. DOI: 10.1016/j.cell.2004.12.020 [PubMed: 15707899]

Chu Y, Hughes S, Chan-Ling T. Differentiation and migration of astrocyte precursor cells and astrocytes in human fetal retina: relevance to optic nerve coloboma. FASEB J. 2001; 15(11):2013–2015. DOI: 10.1096/fj.00-0868fje [PubMed: 11511521]

DiMaio TA, Sheibani N. PECAM-1 isoform-specific functions in PECAM-1-deficient brain microvascular endothelial cells. Microvasc Res. 2008; 75(2):188–201. DOI: 10.1016/j.mvr.2007.10.001 [PubMed: 18029285]

Distler C, Dreher Z, Stone J. Contact spacing among astrocytes in the central nervous system: An hypothesis of their structural role. Glia. 1991; 4:484–494. [PubMed: 1834565]

Dorrell MI, Aguilar E, Friedlander M. Retinal vascular development is mediated by endothelial filopodia, a preexisting astrocytic template and specific R-cadherin adhesion. Invest Ophthalmol Vis Sci. 2002; 43(11):3500–3510. [PubMed: 12407162]

Dorrell MI, Aguilar E, Jacobson R, Trauger SA, Friedlander J, Siuzdak G, Friedlander M. Maintaining retinal astrocytes normalizes revascularization and prevents vascular pathology associated with oxygen-induced retionpathy. Glia. 2010; 58:43–54. [PubMed: 19544395]

Fantes J, Ragge NK, Lynch SA, McGill NI, Collin JR, Howard-Peebles PN, … FitzPatrick DR. Mutations in SOX2 cause anophthalmia. Nat Genet. 2003; 33(4):461–463. DOI: 10.1038/ng1120 [PubMed: 12612584]

Fruttiger M. Development of the mouse retinal vasculature: angiogenesis versus vasculogenesis. Invest Ophthalmol Vis Sci. 2002; 43(2):522–527. [PubMed: 11818400]

Fruttiger M, Calver AR, Kruger WH, Mudhar HS, Michalovich D, Takakura N, … Richardson WD. PDGF mediates a neuron-astrocyte interaction in the developing retina. Neuron. 1996; 17(6):1117–1131. [PubMed: 8982160]

Gerhardt H, Golding M, Fruttiger M, Ruhrberg C, Lundkvist A, Abramsson A, … Betsholtz C. VEGF guides angiogenic sprouting utilizing endothelial tip cell filopodia. J Cell Biol. 2003; 161(6):1163–1177. DOI: 10.1083/jcb.200302047 [PubMed: 12810700]

Giocanti-Auregan A, Vacca O, Benard R, Cao S, Siqueiros L, Montanez C, … Tadayoni R. Altered astrocyte morphology and vascular development in dystrophin-Dp71-null mice. Glia. 2016; 64(5):716–729. DOI: 10.1002/glia.22956 [PubMed: 26711882]

Gnanaguru G, Bachay G, Biswas S, Pinzon-Duarte G, Hunter DD, Brunken WJ. Laminins containing the beta2 and gamma3 chains regulate astrocyte migration and angiogenesis in the retina. Development. 2013; 140(9):2050–2060. DOI: 10.1242/dev.087817 [PubMed: 23571221]

Hollander H, Makarov F, Dreher Z, van Driel D, Chan-Ling TL, Stone J. Structure of the macroglia of the retina: sharing and division of labour between astrocytes and Muller cells. J Comp Neurol. 1991; 313(4):587–603. DOI: 10.1002/cne.903130405 [PubMed: 1783683]

Jiang B, Bezhadian MA, Caldwell RB. Astrocytes modulate retinal vasculogenesis: effects on endothelial cell differentiation. Glia. 1995; 15(1):1–10. DOI: 10.1002/glia.440150102 [PubMed: 8847096]

Kiefer JC. Back to basics: Sox genes. Dev Dyn. 2007; 236(8):2356–2366. DOI: 10.1002/dvdy.21218 [PubMed: 17584862]

Koike T, Wakabayashi T, Mori T, Hirahara Y, Yamada H. Sox2 promotes survival of satellite glial cells in vitro. Biochem Biophys Res Commun. 2015; 464(1):269–274. DOI: 10.1016/j.bbrc.2015.06.141 [PubMed: 26116536]

Kubota Y, Hirashima M, Kishi K, Stewart CL, Suda T. Leukemia inhibitory factor regulates microvessel density by modulating oxygen-dependent VEGF expression in mice. J Clin Invest. 2008; 118(7):2393–2403. DOI: 10.1172/JCI34882 [PubMed: 18521186]

Kubota Y, Suda T. Feedback mechanism between blood vessels and astrocytes in retinal vascular development. Trends Cardiovasc Med. 2009; 19(2):38–43. DOI: 10.1016/j.tcm.2009.04.004 [PubMed: 19577710]

Liesi P, Silver J. Is astrocyte laminin involved in axon guidance in the mammalian CNS? Dev Biol. 1988; 130(2):774–785. [PubMed: 3143614]

Ling TL, Mitrofanis J, Stone J. Origin of retinal astrocytes in the rat: evidence of migration from the optic nerve. J Comp Neurol. 1989; 286(3):345–352. DOI: 10.1002/cne.902860305 [PubMed: 2768562]

Liu YR, Laghari ZA, Novoa CA, Hughes J, Webster JR, Goodwin PE, … Scotting PJ. Sox2 acts as a transcriptional repressor in neural stem cells. BMC Neurosci. 2014; 15:95.doi: 10.1186/1471-2202-15-95 [PubMed: 25103589]

Luna G, Keeley PW, Reese BE, Linberg KA, Lewis GP, Fisher SK. Astrocyte structural reactivity and plasticity in models of retinal detachment. Exp Eye Res. 2016; 150:4–21. DOI: 10.1016/j.exer.2016.03.027 [PubMed: 27060374]

Macosko EZ, Basu A, Satija R, Nemesh J, Shekhar K, Goldman M, … McCarroll SA. Highly parallel genome-wide expression profiling of individual cells using nanoliter droplets. Cell. 2015; 161(5): 1202–1214. DOI: 10.1016/j.cell.2015.05.002 [PubMed: 26000488]

Matsushima D, Heavner W, Pevny LH. Combinatorial regulation of optic cup progenitor cell fate by SOX2 and PAX6. Development. 2011; 138(3):443–454. DOI: 10.1242/dev.055178 [PubMed: 21205789]

Mi H, Haeberle H, Barres BA. Induction of astrocyte differentiation by endothelial cells. J Neurosci. 2001; 21(5):1538–1547. [PubMed: 11222644]

Molofsky AV, Krencik R, Ullian EM, Tsai HH, Deneen B, Richardson WD, … Rowitch DH. Astrocytes and disease: a neurodevelopmental perspective. Genes Dev. 2012; 26(9):891–907. DOI: 10.1101/gad.188326.112 [PubMed: 22549954]

Nakashima K, Yanagisawa M, Arakawa H, Taga T. Astrocyte differentiation mediated by LIF in cooperation with BMP2. FEBS Lett. 1999; 457(1):43–46. [PubMed: 10486560]

Newman EA. High potassium conductance in astrocyte endfeet. Science. 1986; 233(4762):453–454. [PubMed: 3726539]

O'Sullivan ML, Punal VM, Kerstein PC, Brzezinski JA, Glaser T, Wright KM, Kay JN. Astrocytes follow retinal ganglion cells axons to establish an angiogenic template during retinal development. Glia. 2017; 65(10):1687–1716. DOI: 10.1002/glia.23189

Provis JM, Leech J, Diaz CM, Penfold PL, Stone J, Keshet E. Development of the human retinal vasculature: cellular relations and VEGF expression. Exp Eye Res. 1997; 65(4):555–568. DOI: 10.1006/exer.1997.0365 [PubMed: 9464188]

Ramirez JM, Trivino A, Ramirez AI, Salazar JJ, Garcia-Sanchez J. Structural specializations of human retinal glial cells. Vision Res. 1996; 36(14):2029–2036. [PubMed: 8776469]

Ruhrberg C, Gerhardt H, Golding M, Watson R, Ioannidou S, Fujisawa H, … Shima DT. Spatially restricted patterning cues provided by heparin-binding VEGF-A control blood vessel branching morphogenesis. Genes Dev. 2002; 16(20):2684–2698. DOI: 10.1101/gad.242002 [PubMed: 12381667]

Sandercoe TM, Madigan MC, Billson FA, Penfold PL, Provis JM. Astrocyte proliferation during development of the human retinal vasculature. Exp Eye Res. 1999; 69(5):511–523. DOI: 10.1006/exer.1999.0730 [PubMed: 10548471]

Sarthy PV, Fu M, Huang J. Developmental expression of the glial fibrillary acidic protein (GFAP) gene in the mouse retina. Cell Mol Neurobiol. 1991; 11(6):623–637. [PubMed: 1723659]

Schafer DP, Lehrman EK, Kautzman AG, Koyama R, Mardinly AR, Yamasaki R, … Stevens B. Microglia sculpt postnatal neural circuits in an activity and complement-dependent manner. Neuron. 2012; 74(4):691–705. DOI: 10.1016/j.neuron.2012.03.026 [PubMed: 22632727]

Schneider A, Bardakjian T, Reis LM, Tyler RC, Semina EV. Novel SOX2 mutations and genotype-phenotype correlation in anophthalmia and microphthalmia. Am J Med Genet A. 2009; 149A(12): 2706–2715. DOI: 10.1002/ajmg.a.33098 [PubMed: 19921648]

Sofroniew MV, Vinters HV. Astrocytes: biology and pathology. Acta Neuropathol. 2010; 119(1):7–35. DOI: 10.1007/s00401-009-0619-8 [PubMed: 20012068]

Stevens B, Allen NJ, Vazquez LE, Howell GR, Christopherson KS, Nouri N, … Barres BA. The classical complement cascade mediates CNS synapse elimination. Cell. 2007; 131(6):1164–1178. DOI: 10.1016/j.cell.2007.10.036 [PubMed: 18083105]

Stone J, Dreher Z. Relationship between astrocytes, ganglion cells and vasculature of the retina. J Comp Neurol. 1987; 255(1):35–49. DOI: 10.1002/cne.902550104 [PubMed: 3819008]

Stone J, Itin A, Alon T, Pe'er J, Gnessin H, Chan-Ling T, Keshet E. Development of retinal vasculature is mediated by hypoxia-induced vascular endothelial growth factor (VEGF) expression by neuroglia. J Neurosci. 1995; 15(7 Pt 1):4738–4747. [PubMed: 7623107]

Surzenko N, Crowl T, Bachleda A, Langer L, Pevny L. SOX2 maintains the quiescent progenitor cell state of postnatal retinal Muller glia. Development. 2013; 140(7):1445–1456. DOI: 10.1242/dev.071878 [PubMed: 23462474]

Tao C, Zhang X. Development of astrocytes in the vertebrate eye. Dev Dyn. 2014; 243(12):1501–1510. DOI: 10.1002/dvdy.24190 [PubMed: 25236977]

Taranova OV, Magness ST, Fagan BM, Wu Y, Surzenko N, Hutton SR, Pevny LH. SOX2 is a dose-dependent regulator of retinal neural progenitor competence. Genes Dev. 2006; 20(9):1187–1202. DOI: 10.1101/gad.1407906 [PubMed: 16651659]

Ullian EM, Sapperstein SK, Christopherson KS, Barres BA. Control of synapse number by glia. Science. 2001; 291(5504):657–661. DOI: 10.1126/science.291.5504.657 [PubMed: 11158678]

Watanabe T, Raff MC. Retinal astrocytes are immigrants from the optic nerve. Nature. 1988; 332(6167):834–837. DOI: 10.1038/332834a0 [PubMed: 3282180]

West H, Richardson WD, Fruttiger M. Stabilization of the retinal vascular network by reciprocal feedback between blood vessels and astrocytes. Development. 2005; 132(8):1855–1862. DOI: 10.1242/dev.01732 [PubMed: 15790963]

Whitney IE, Keeley PW, St John AJ, Kautzman AG, Kay JN, Reese BE. Sox2 regulates cholinergic amacrine cell positioning and dendritic stratification in the retina. J Neurosci. 2014; 34(30):10109–10121. DOI: 10.1523/JNEUROSCI.0415-14.2014 [PubMed: 25057212]

Zhang Y, Chen K, Sloan SA, Bennett ML, Scholze AR, O'Keeffe S, … Wu JQ. An RNA-sequencing transcriptome and splicing database of glia, neurons, and vascular cells of the cerebral cortex. J Neurosci. 2014; 34(36):11929–11947. DOI: 10.1523/JNEUROSCI.1860-14.2014 [PubMed: 25186741]

Zhang Y, Porat RM, Alon T, Keshet E, Stone J. Tissue oxygen levels control astrocyte movement and differentiation in developing retina. Brain Res Dev Brain Res. 1999; 118(1–2):135–145. [PubMed: 10611512]

Main Points

Sox2 is necessary for the proper time course of astrocyte maturation and angiogenesis.

Sox2-deficient astrocytes display aberrant morphology in adulthood.

The vasculature is underdeveloped in Sox2 conditional knockout retinas.

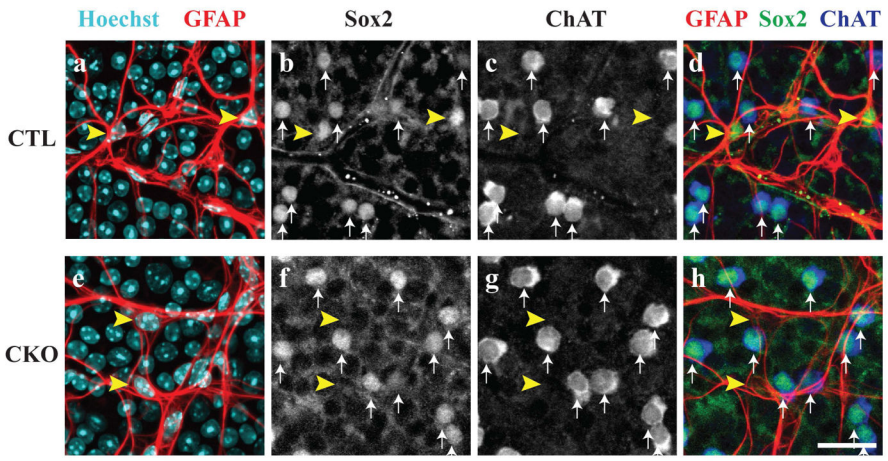

Figure 1. Characterization of Sox2 conditional knockout mice

In control animals (CTL), astrocytes are visualized by co-localization of Hoechst and GFAP antibodies (yellow arrowheads, a). These cells are distinct from cholinergic amacrine cells that are both ChAT and Sox2-positive (white arrows, b–d). In the *Sox2* conditional knockout retinas (CKO), astrocytes are Sox2-deficient as evidenced by the lack of Sox2 staining in astrocyte cell bodies (yellow arrowheads, e–f, h). However, Sox2 remains in cholinergic amacrine cells (white arrows, f–h), showing that Sox2 is removed only from the population of retinal astrocytes. Scale bar = 25 μm.

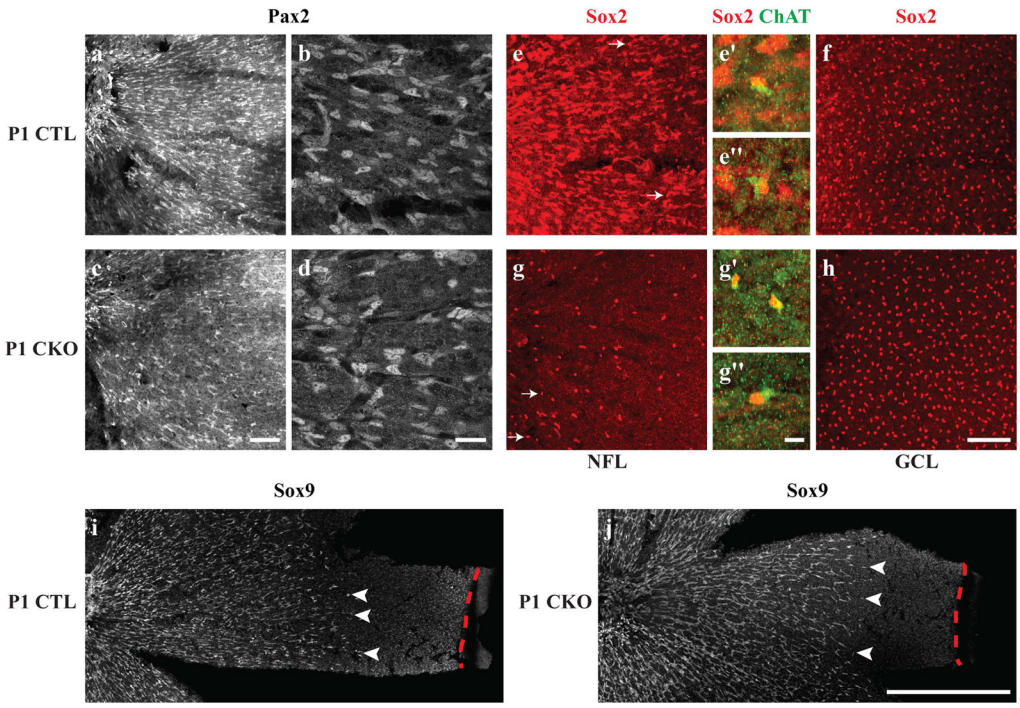

Figure 2. Astrocytes at P1 migrate normally in CKO retinas, despite lacking Sox2

The migrating wave of astrocytes in both the CTL and CKO retinas, labeled with Pax2, extends from the ONH to about two-thirds of the distance to the retinal margin (a,c). At higher magnification, CTL Pax2-positive astrocytes that are migrating from the ONH in the central retina (left) exhibit an elongated morphology typical of migrating astrocytes (b). CKO Pax2-positive cells appear in comparable density and morphology to CTL retinas (c–d). Almost all Sox2-immunopositive cells in the NFL appear to be astrocytes, with the exception of a few ChAT-positive cells that are occasionally found in the NFL (arrows in e,e′,e″), yet are spatially displaced from the population of Sox2-positive cholinergic amacrine cells in the GCL (f). In CKO retinas, by contrast, very few Sox2-positive cells are found in the NFL (g) and are displaced ChAT-positive cells (g′ and g″). The population of cholinergic amacrine cells in the GCL appears indistinguishable from CTL retinas (h). P1 CTL (i) and CKO (j) retinas were labeled with another astrocytic marker, Sox9, that supports the findings in a–d, that immature astrocytes migrate comparable distances in CTL and CKO retinas (arrowheads indicate the furthest migrating Sox9+ nuclei, while red dashed lines indicate the retinal margin). All panels are oriented with the ONH to the left. Scale bar: a,c,e,f,g,h = 100 μm; b,d = 25 μm; e′,e″,g′,g″ = 10 μm; i,j, = 500 μm.

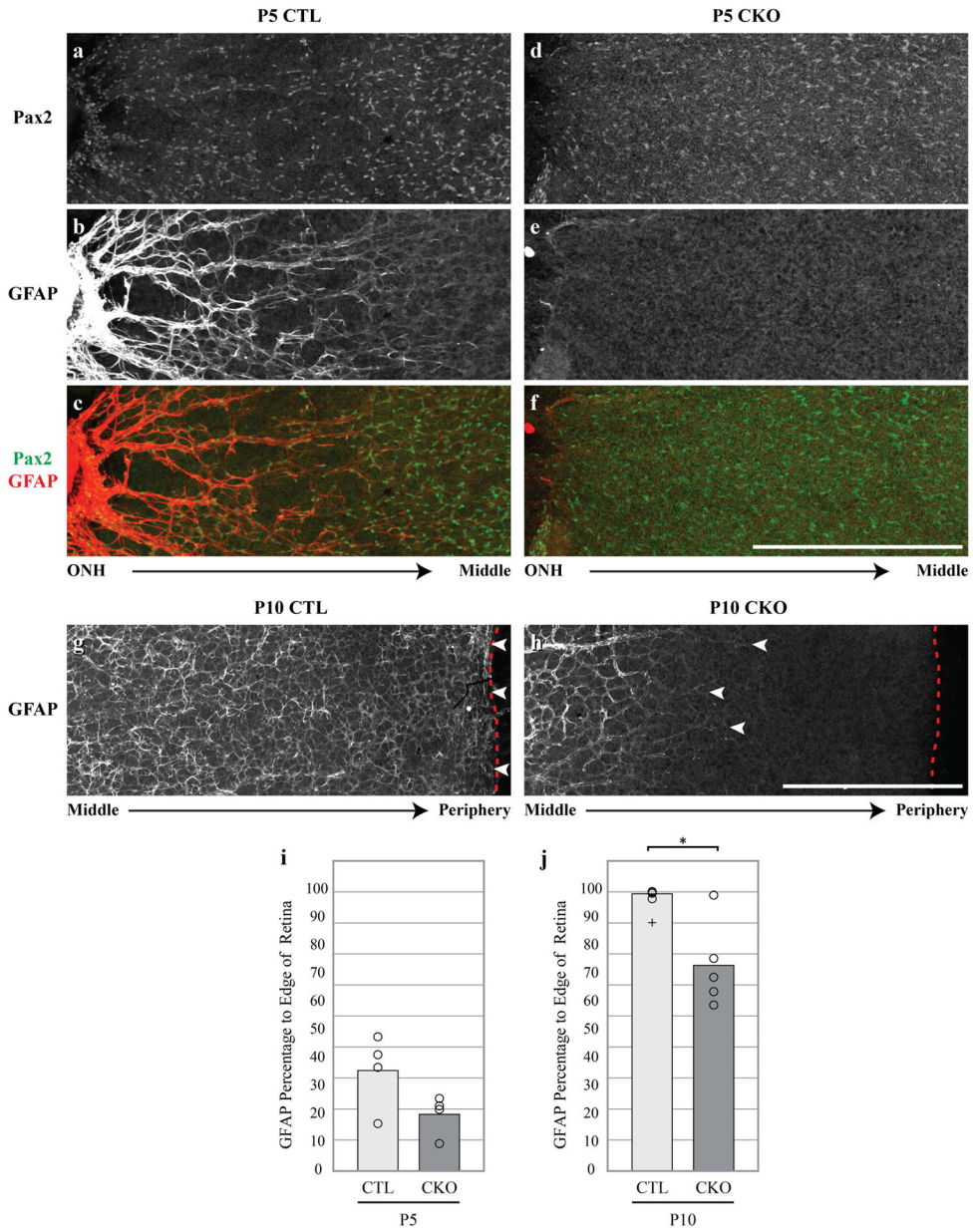

Figure 3. CKO retinas exhibit a delayed maturation at P5 and P10

CTL Pax2-positive astrocytes at P5 are arranged in a ring-like pattern (a) and upregulate GFAP robustly near the ONH (b). In this region, the distribution of Pax2-positive cells coincides with the GFAP network (c). Conversely, CKO astrocyte cell bodies do not rearrange themselves as they do in CTLs, evidenced by their more uniform distribution (d). CKO astrocytes also exhibit a delayed GFAP upregulation peripherally (e,f,j, CTL: n = 4, CKO: n = 4). At P10, GFAP-positive astrocyte processes (g, arrowheads) nearly reach the far peripheral margin of the retina (g, dashed line). Processes closer to the central retina become thinner and begin forming the web-like morphology characteristic of GFAP-positive processes seen in mature CTL retinas (g). In P10 CKO retinas however, the extension of GFAP-positive processes (h, arrowheads) is significantly delayed, usually failing to reach the

retinal margin (h, red dashed line) by this age (j, CTL: n = 4, CKO: n = 5). In addition, GFAP-positive processes at more central locations show a delay in their acquisition of the more mature patterning exhibited in CTL retinas (h). Cross in j represents an outlier not included in the statistical analysis. Scale bar = 500 μm. * = $p \leq .05$.

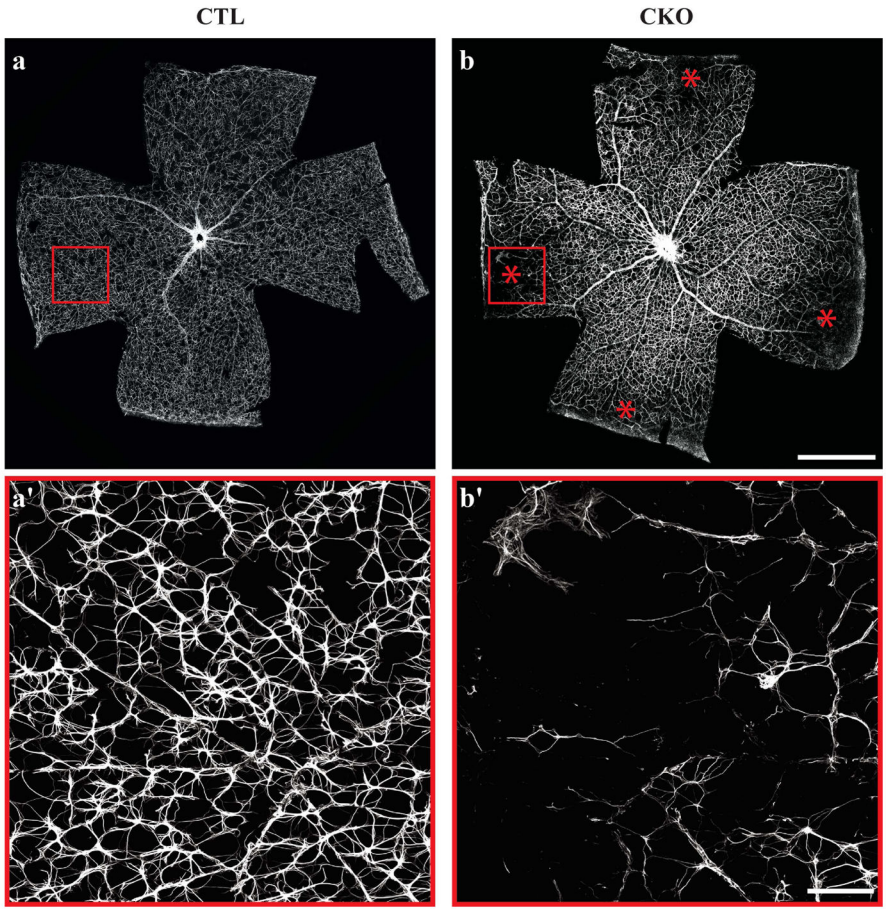

Figure 4. Peripheral retinas display regions of GFAP-depletion

CTL astrocytes exhibit a uniform GFAP staining pattern across the surface of the retina (a). Magnification of the area within the red box in a demonstrates the characteristic web of GFAP-positive processes (a′). CKO retinas show a regional loss of GFAP staining in peripheral retina (b). Magnification of red box in b (b′). * = Quadrants with loss of GFAP immunoreactivity. Scale bar a–b = 1 mm; a′–b′ = 100 μm.

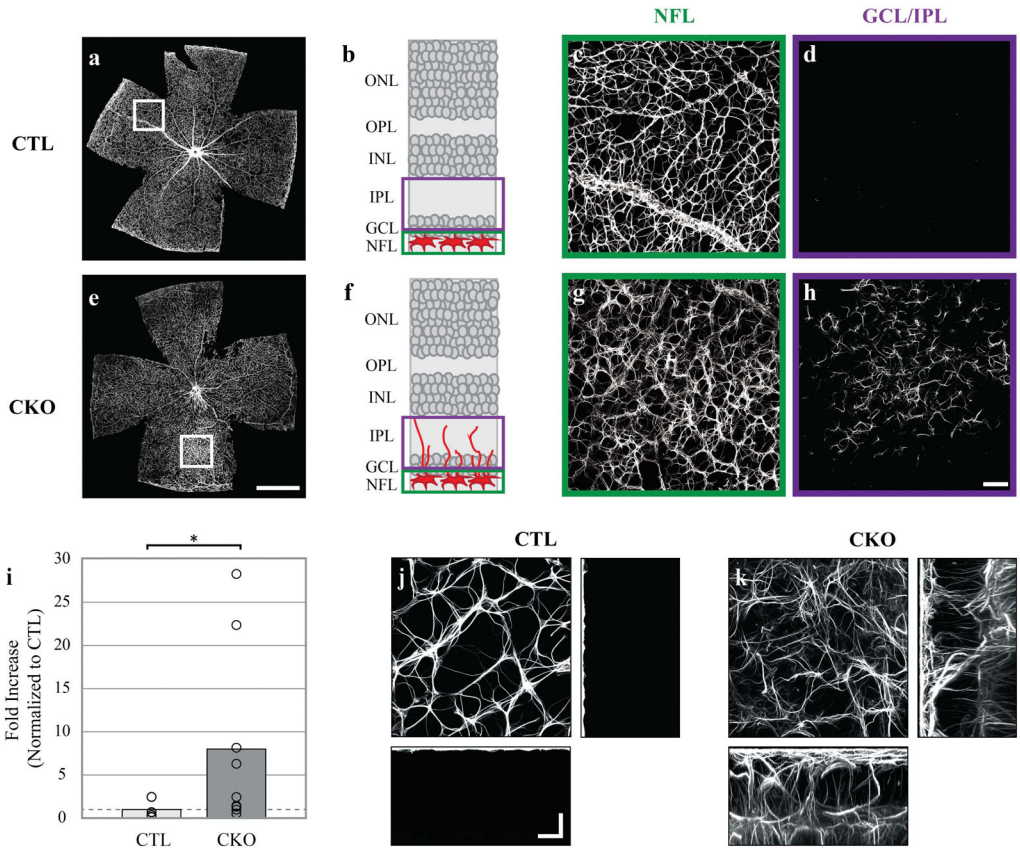

Figure 5. GFAP processes sprout into the inner retina in CKO animals

Whole CTL retina immunostained with GFAP (a). Schematic of retinal section showing that GFAP-positive astrocytic processes are almost exclusively confined to the NFL (green box, b). GFAP staining is uniform across the NFL when viewing a field *en face* (c, magnified from white box in a). The GCL and IPL are largely devoid of GFAP labeling in CTL retinas (d). Whole CKO retina stained with GFAP (e). Schematic of retinal section depicts GFAP-positive processes extending into the retina past the GCL (purple box, f). GFAP staining is uniform across the NFL in this example, as in CTL retinas (g), yet CKO retinas display sprouting of processes well beyond the level of their normal positioning (h, magnified from white box in e). Sprouting is extensive in the CKO retinas relative to CTL retinas (i, dashed line represents CTL retinas normalized to 1; CTL: n = 8, CKO: n = 9). High magnification z-stack reconstruction from CTL retina showing no astrocytic labeling extending into the inner retina (j). High magnification z-stack reconstruction from CKO retina showing aberrant sprouting into the inner retina extending at least 120 μm deep (k). Scale bar a,e = 1 mm; c,d,g,h = 100 μm, j,k = 25 μm. * = $p \leq .05$.

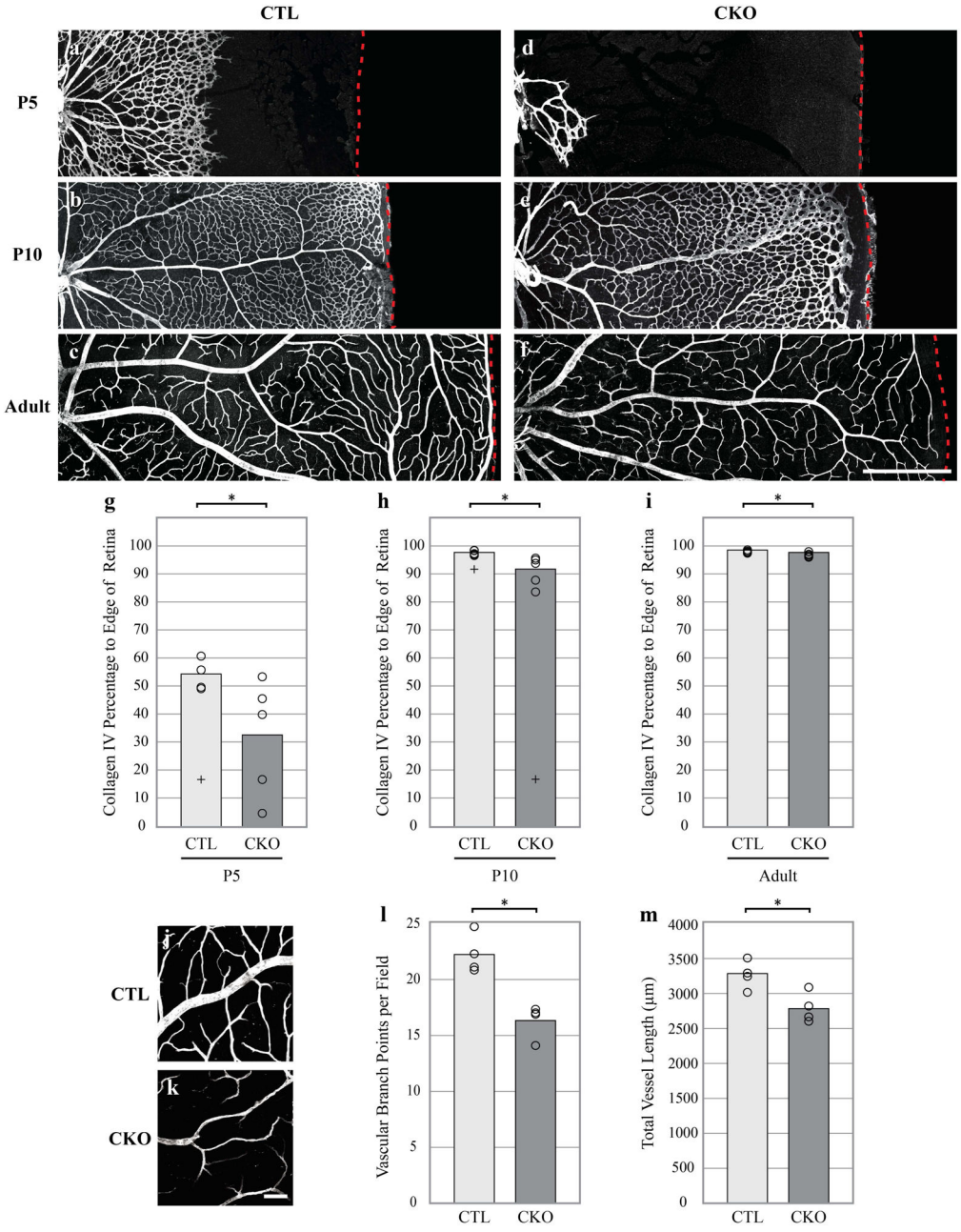

Figure 6. Retinal vasculature develops abnormally in CKO retinas

Representative images showing extent of vascular outgrowth in CTL retinas (a–c) and CKO (d–f) at P5, P10, and adult (P22), respectively. At P5, CKO retinas show a significant decrease in the invasion of Collagen IV-positive blood vessels as evidenced by a marked decrease in the percentage of their extension to the retinal margin compared to CTL retinas (g, CTL: n = 4, CKO: n = 5). CKO vascular invasion still shows a delay at P10 (h, CTL: n = 5, CKO: n = 5) and this difference is sustained into adulthood when CKO retinas show a significant reduction in the extension of the vascular network towards the peripheral margin (i, CTL: n = 5, CKO: n = 5). Representative fields from adult CTL (h) and CKO (i) retinas

stained with Collagen IV reveal that CKO retinas have significantly fewer vascular branch points (j, CTL: n = 4, CKO: n = 4) and an overall decrease in total vessel length per field than CTL retinas (k, CTL: n = 4, CKO: n = 4). Dashed red line represents the retinal margin. Panels in a–f are oriented with ONH to left. In the histograms in panel g, open circles represent individual retinas and crosses were outliers not included in analysis. Scale bar a–f = 500 μm mm; h,i = 100 μm. * = $p \leq .05$.

Table 1

Primary antibodies used in the present study.

Antibody	Supplier	Catalog Number	Dilution
Mouse αGFAP (conjugated to Cy3)	Sigma-Aldrich	C9205	1:400
Rabbit αPax2	Biolegend	901001	1:200
Rabbit αCollagen IV	BioRad ABD Serotec	2150-1470	1:1,000
Goat αChAT	Millipore	AB144P	1:50
Rabbit αSox2	Abcam	ab97959	1:200
Goat αSox9	R&D Systems	AF3075	1:2,000
Mouse αCtBP2	BD Transduction Laboratories	612044	1:500
Sheep αTH	Millipore	AB152	1:10,000
Mouse αPKARIIβ	BD Transduction Laboratories	610625	1:1,000
Rabbit αNeurofilament M 145kD	Millipore	AB1987	1:1,000
Rabbit αIba1	Wako	019-19741	1:1,000
Mouse αPKC	Millipore	05-983	1:500
Rabbit αmCAR	Millipore	AB15282	1:5,000
Mouse αSMI32	Covance	SMI32R	1:200
Rabbit αCalbindin	Millipore	PC253L	1:10,000
Mouse αSyt2	Santa Cruz Biotechnologies	SC6026	1:250
Goat αVGluT3	Santa Cruz Biotechnologies	SC26031	1:500
Mouse αCre Recombinase	Millipore	MAB3120	1:1,000
Chicken αVimentin	Millipore	AB5733	1:1,000